

Effect of Three-Dimensional Geometry on the Sloshing Behavior of Rectangular Concrete Tanks



I. Tavakkoli Avval

Department of Civil Engineering, Ryerson University, Canada

M.R. Kianoush

Department of Civil Engineering, Ryerson University, Canada

A.R. Ghaemmaghami

CANDU Energy Inc., Canada

SUMMARY:

The effect of three-dimensional geometry on the seismic response of open-top rectangular concrete water tanks is investigated. In this study, the fluid-structure interaction is introduced incorporating wall flexibility. Numerical studies are done based on finite element simulation of the tank-liquid system. The ANSYS finite element program is used in this study. The liquid-tank system is modelled assuming both 2D and 3D geometries. Parametric studies are conducted to investigate the effect of parameters such as water depth and tank configuration on sloshing response. Due to three-dimensional geometry, amplification of the dynamic response in the form of sloshing height is observed. It is shown that at the corner of the tanks, the interaction of the waves generated in longitudinal and transverse directions initiates greater wave amplitude.

Keywords: Seismic response, rectangular tank, concrete, sloshing, three-dimensional modelling

1. GENERAL OVERVIEW ON LIQUID CONTAINING STRUCTURES

One of the critical lifeline structures, which have become widespread during the recent decades, is liquid containing structure. Liquid containing structures (LCS) are used for storage of water, petroleum products, oxygen, nitrogen, high-pressure gas, Liquefied Natural Gas (LNG), Liquefied Petroleum Gas (LPG), and etc. There are many types of such storage tanks depending on the structure, construction material, content, volume, and storage condition. Liquid storage tanks can be constructed by steel or concrete. Due to excessive damages reported on steel tank, the concrete storage tanks have become very popular. Reinforced Concrete (RC) has been used in environmental engineering structures such as water reservoirs and sewage treatment tanks. Water tanks are in demand for the storage of drinking water, fire suppression, agricultural farming and livestock, food preparation and many other applications. These structures may provide services necessary for the emergency response of a community after an earthquake. It is worth mentioning here that reinforced concrete tanks are designed for functionality during the normal life cycle; moreover, reinforced concrete tanks should withstand the earthquake loading without any excessive cracking.

It should be noted that the seismic design of the liquid storage tanks requires knowledge of natural frequencies, hydrodynamic pressure distribution on the walls, resulting forces and moment as well as the sloshing of the contained liquid. These parameters have direct effect on the dynamic stability and performance of the excited containers. The dynamic behaviour of the water tanks is governed by the interaction between the fluid and the structure, and structure flexibility plays an important factor that should be properly addressed. The effect of fluid interaction on the seismic response of the rectangular water tanks has been the subject of many studies in the past several years. For instance, Livaoglu (2008) structured a research on this topic. However, most of the studies are concentrated on the effect of fluid interaction on the cylindrical tanks and only a small number of them are focused on the evaluating the effect of fluid-structure interaction on the seismic response of the rectangular tanks.

Three-dimensional geometry and restraint condition are also matter of crucial concerns that need to be

addressed in the design procedure of the rectangular water tank. Ghaemmaghami and Kianoush (2010) conducted intensive research on the dynamic time-history responses of the rectangular tanks. In their study, the responses of the rigid tanks were compared with the identical case of flexible tank. Significant amplifications in the structural responses were perceived. They also investigated the effect of the 3D geometry for two different tank configurations.

Koh et al. (1998) directed thorough research on the effect of the 3D restraint condition on the dynamic behaviour of the rectangular tank using Boundary Element and Finite Element Method (BEM-FEM). They also investigated the sloshing behaviour of the externally excited rectangular tank and compared their outcome with experimental test result.

Sloshing is defined as any motion of the free liquid surface inside its container and it is caused by any disturbance to a partially filled liquid container. The problems of liquid sloshing effects on large dams, water reservoirs, elevated water tanks, and oil tanks always have been matter of concern of civil engineers. The sloshing displacement of the fluid is profoundly important at the service level and for the design of tank roofs. This study is focused on the effect of sloshing in rectangular tanks.

1.1. Scope and Objectives

In spite of wide range of studies on the dynamic response of the rectangular water tanks, many parameters need to be addressed for a better design of LCS subjected to base excitation. Additional factors that should be directed include wall flexibility, three-dimensional geometry, direction of the ground motion and the full time-domain simulation. In this context, the primary objective of the present work are to investigate; first, the effect of three-dimensional geometry on the structural responses; second, the wave amplitude at the critical locations of the three-dimensional tanks for free-board design; finally, the sloshing height at the corner of the rectangular tanks subjected to the multi component excitation.

Flexibility of the wall is addressed in this study to predict the dynamic responses. This study is limited to the linear elastic analysis of the open-top rectangular tanks that are anchored at the base and filled with water. Tanks are assumed to be fixed to a rigid foundation; therefore, the effect of soil-structure interaction is ignored. Tanks walls are considered to have constant thickness. Small wave amplitude or linear wave theory is used for evaluating the seismic performance of the LCS. For this purpose, finite element program, ANSYS with fluid-structure interaction analysis capabilities, is used for the dynamic time history analysis. The result of the present work can be used for code and standard developments. It is an approach to identifying, assessing and reducing the risks of disaster and it will aim to reduce social-economical vulnerabilities to earthquake.

2. MATHEMATICAL BACKGROUND

Fig. 2.1 shows a schematic diagram of the liquid-tank system under coordinate system. A rectangular water tank of a and b dimensions, partially filled with water to the depth of h . Owing to the three-dimensional geometry of the problem, a Cartesian coordinate system is employed to describe the position of any point belonging to the liquid domain. The container is assumed to be fixed to the rigid ground and the Cartesian co-ordinate system (x, y, z) has the origin located at the centre of the container, with oz opposing the direction of gravity and $z=h/2$ coinciding the free surface of water.

2.1. Governing Equations

If the tanks is assumed to be attached to a rigid base and the contained fluid is inviscid and incompressible resulting in an irrotational flow field, the velocity potential Φ contains of x , y and z components of u , v and w , which are computed of spatial derivation of the velocity potential:

$$u = \frac{\partial \phi}{\partial t} \quad v = \frac{\partial \phi}{\partial t} \quad w = \frac{\partial \phi}{\partial t} \quad (2.1)$$

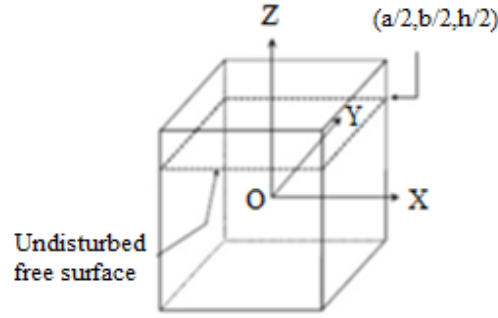


Figure 2.1. Coordinate system used for derivation of sloshing equations

The velocity potential should satisfy the 3-D Laplace equation at any point of the liquid domain, respecting the assumption of incompressible fluid:

$$\frac{\partial u}{\partial t} + \frac{\partial v}{\partial t} + \frac{\partial w}{\partial t} = 0 \quad \text{or} \quad \nabla^2 \phi = 0 \quad (2.2)$$

For the inviscid fluid with either steady or unsteady flow, the equations of momentum conservation may be integrated to yield a single scalar equation referred to as Bernoulli's equation:

$$\frac{\partial \phi}{\partial t} + \frac{P}{\rho_l} + gz + \frac{1}{2}(u^2 + v^2 + w^2) = f(t) \quad (2.3)$$

Where P is pressure, ρ_l is fluid density, and g is the acceleration due to gravity corresponding to negative z direction. $f(t)$ is the constant of the integration. As u , v and w components of velocity are assumed to be small, squared value of these quantities are also small compared to first order values and can be neglected. As a result, if the constant value of $f(t)$ can be observed into Φ , the Bernoulli's equation will be linearized to the following form:

$$\frac{\partial \phi}{\partial t} + \frac{P}{\rho_l} + gz = 0 \quad (2.4)$$

Assuming $\eta(x,y,t)$ sloshing displacement to be very small and using the small wave theory, the linearized boundary condition at the free surface may also be written to Eqn. 2.5.

$$\frac{1}{g} \frac{\partial^2 \phi}{\partial t^2} + \frac{\partial \phi}{\partial z} = 0 \quad z = h/2 \quad (2.5)$$

The surface is free to move and $P = \rho g \eta$ at $z = h/2$; so, again if $\eta(x,y,t)$ represents the small displacement of the liquid, the unsteady Bernoulli equation can be written as:

$$\frac{\partial \phi(x,y,t)}{\partial t} + g\eta(x,y,t) = 0 \quad z = h/2 \quad (2.6)$$

In addition to dynamic boundary condition, the kinematic boundary condition also should be satisfied. Accordingly, liquid at the free surface always remains at the free surface. The kinematic boundary condition at the free surface relates the surface displacement to the vertical component of the velocity at the surface, and this equation forms as:

$$\frac{\partial \eta}{\partial t} = \frac{\partial \phi}{\partial z} = w \quad (2.7)$$

At the wet surface of the tank, the fluid velocity in the direction perpendicular to the tanks wall should be equal to the tanks velocity, $v_n(t)$, perpendicular to walls own plane (n stands for the normal direction). Note that this assumption is only applicable for the cases that the tank motion is not rotational and if the viscous stresses are negligible.

$$\frac{\partial \phi}{\partial n} = v_n(t) \quad (2.8)$$

For the tanks with rigid walls, $v_n(t)$ equals to grounds velocity. For the case of flexible walls, walls velocity is the summation of the ground velocity and its relative velocity due to wall flexibility.

2.2. Finite Element Formulation

For a coupled system, such as the one of concern in this study, there are unknown forces at the interface. As a result, neither of the domains can be solved independently of the other. In a partially filled water tank, coupling occurs on domain interfaces via the boundary conditions. In these cases, physically different problems interact, but it is possible to consider coupling between the domains that are physically similar.

If the system is subjected to base acceleration of $[\ddot{u}_g]$, the equation of motion for the tank structure shall be written according to Eqn. 2.9, where M , C and K , respectively, are mass, damping and stiffness matrices for the structure domain.

$$[M][\ddot{u}] + [C][\dot{u}] + [K][u] = f_t - [M][\ddot{u}_g] \quad (2.9)$$

In Eqn. 2.9, $[\ddot{u}]$ is the acceleration vector of the nodes at the boundary element in the structural domain, and $[\ddot{u}_g]$ is the ground acceleration vector applied to the system. Equation of motion for the liquid domain can be expressed as Eqn. 2.10. In this equation, $[Q]$ is the coupling matrix that relates the pressure of the liquid to the equivalent nodal structural forces and reverse. $[P]$ is the pressure vector acting on the interface element. Likewise, $[M']$, $[C']$ and $[K']$ are the mass matrix, damping and stiffness matrices for the fluid domain, respectively.

$$[M'][\ddot{P}] + [C'][\dot{P}] + [K'][P] = [F_2] - \rho[Q]^T[\ddot{u}] \quad (2.10)$$

To calculate pressure and displacement and their derivation at each time step, Newmark's method is employed in this study.

3. FINITE ELEMENT IMPELMENTATION

The rectangular concrete water tank shown in Fig. 3.1 is the subject of the study. The cross-section parallel to the short side wall is adopted for X direction and the cross section parallel to long side as Y direction. Different tank configurations are modelled in ANSYS program. Material properties for the structure domain and the fluid domain are as follows:

$$\rho_c = 2300 \text{ kg/m}^3 \quad E_c = 26.44 \text{ GPa} \quad \nu = 0.17 \quad \rho_l = 1000 \text{ kg/m}^3 \quad K_l = 2.1 \text{ GPa}$$

where ρ_c , E_c and ν are density, modulus of elasticity and Poisson's ratio for the tank structure, respectively. In addition, ρ_l and K_l represent density and bulk modulus of the contained liquid. For three-dimensional modelling, the tank is assumed to be a symmetric structure with four side flexible walls. It is also assumed that the tank is anchored at its base and the effect of uplift pressure is ignored. The soil-structure effect is neglected. Rectangular tank are called shallow (S), medium (M) and tall (T), respectively, with wall height of 6.0, 8.5 and 12.0 m. Walls thickness are chosen to be 600 mm for

shallow and medium height tanks, and 1200 mm for the tall height tank. Similarly, the bottom slab thickness is 600 mm for the shallow and medium tanks and equals to 1200 mm for the tall tank.

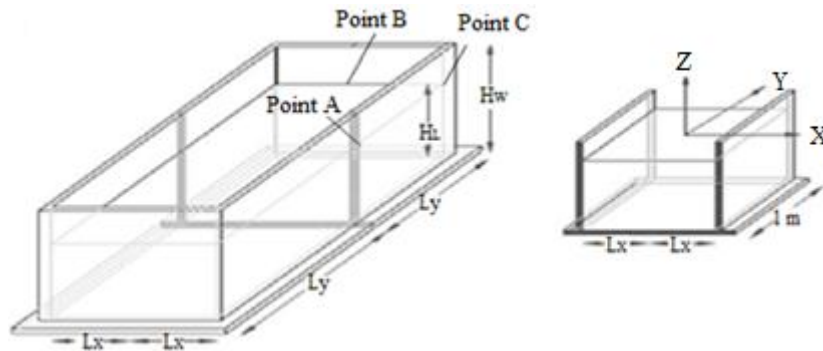


Figure 3.1. Schematic configuration of the rectangular tank

4. SLOSHING CHARACTERISTICS

The seismic response of a half-full rectangular tank under external excitations in both longitudinal and transverse directions is investigated. Time history analysis is conducted to calculate the response of the system at each time step. In this section, the variations of the wave amplitude with time are discussed. For the three-dimensional tank models, the cross-section parallel to the short side wall is adopted for X direction and N-S component of El-Centro (1940) earthquake is applied. The direction parallel to the long wall is adopted for Y direction and is subjected to the E-W component. The components of the earthquake are scaled in such a way that the peak ground acceleration of the N-S component is 0.4g, and that of E-W component is 0.27g. To reduce the computational efforts, analyses are done for the first 20 seconds of the excitation with time intervals of 0.02(s).

The sloshing heights are calculated at the free surface of the water at the middle cross section of the walls in X and Y directions and at the corner of the tank, which are called points A, B and C, respectively. For the 2D analysis, the same division is employed separately for the X and Y directions of the tanks. In the 2D models, the critical point at the free water surface interfacing with the wet surface of the wall is named as point A when the analysis is conducted on the cross-section parallel to the short side wall. Likewise, the point under investigation is named point B when the E-W component of the ground motion is applied parallel to the long side wall.

4.1. Sloshing Height at the Corner of the Rectangular Tanks

In the rectangular tank, the waves generated in X and Y directions, interact at the corner of the tank. This circumstance results in higher sloshing height at the corner of the tank in comparison with sloshing of the water at the middle of the walls. In this study, the sloshing height at the corner of the tank is compared to the sloshing height in both X and Y directions. In this section, three different tank configurations having plan dimensions of 20 m × 40 m are discussed. The depth of water for these tanks are 5.5 m, 8.0 m and 11.0 m and are referred to as S (shallow), M (medium) and T (tall), respectively.

Fig. 4.1 displays the time history of the sloshing behaviour of the three-dimensional model for the case S. It can be observed that the maximum sloshing height of the free surface water in the direction perpendicular to longer dimension (at point A) is 673 mm. The value of the sloshing in the direction parallel to long side wall (at point B) is 475 mm. It is observed that due to applying both longitudinal and transverse component of the earthquake, interaction of the waves initiated a major movement of the surface water at the corner of the tank. The water surface at the corner of the tank shifts about 1067 mm. This value is 58% higher than the displacement at point A. The sloshing height at the corner of the shallow tank is 124% higher than the one at point B.

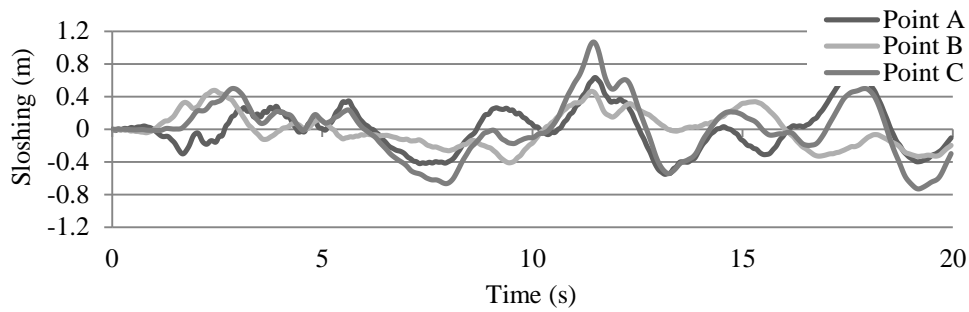


Figure 4.1. Time history of sloshing height for case S

Fig. 4.2 displays the time history sloshing height for the case M. The 3D model estimates sloshing height of 518 mm at point A and 679 mm at point B. The absolute maximum wave shift of 953 mm at the corner of the medium tank occurs at 11.4 s. This value is 84% more than the sloshing height at middle cross section of the long wall at point A. In addition, it is 41% more than the displacement at the middle cross section of the short wall at point B.

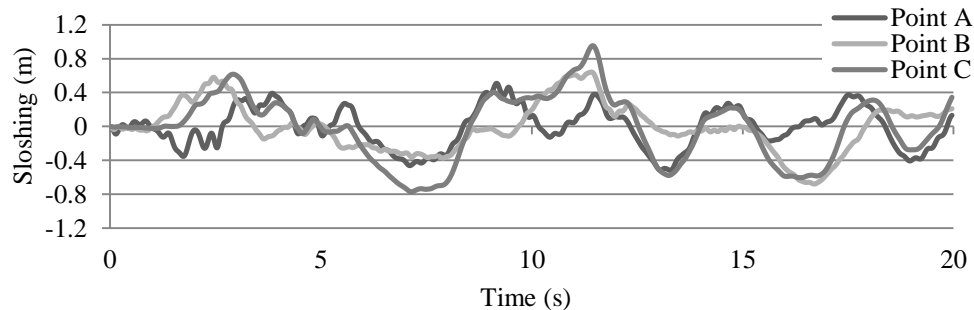


Figure 4.2. Time history of sloshing height for case M

As shown in Fig. 4.3, for the 3D model of the tall tank (T), the free water surface at the middle cross section of the long side wall (Point A) shifts up to 539 mm. The slosh height at point B is 750 mm. Again for the tall tank, wave height at the corner of the tank reaches higher value, and is 86% more than slosh height at point A and 34% more than point B.

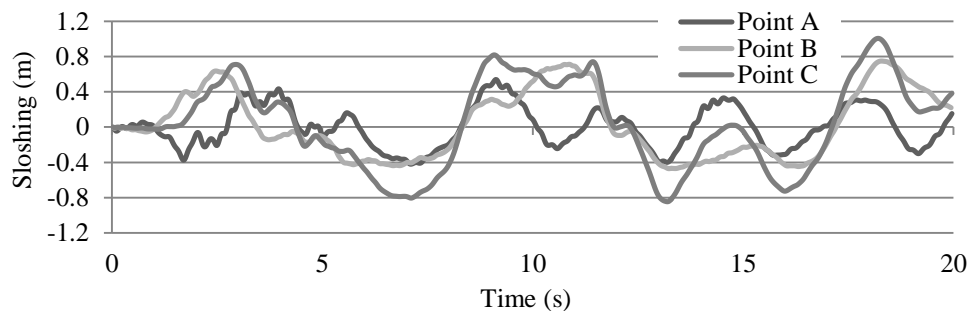


Figure 4.3. Time history of sloshing height for case T

Comparing the results of different tank configurations, it is concluded that in tanks having the same plan dimensions, the sloshing height in both directions increases with water depth. Fig. 4.4 displays the free water surface profile of the maximum sloshing for a typical shallow tank. Due to interaction of the waves in X and Y directions, the peak height is at the corner of the tank. Note that in current practice, two-dimensional models are used to calculate the sloshing height of the seismically excited tank; however, 2D models are unable to predict the slosh height at the corner of the tank, which is significantly higher than other locations. Moreover, in this study, it is observed that for the tanks of the same plan dimensions, the amplification of slosh wave at the corner of the tank relative to the one at the middle of the wall is more profound for the tanks with greater water depth.

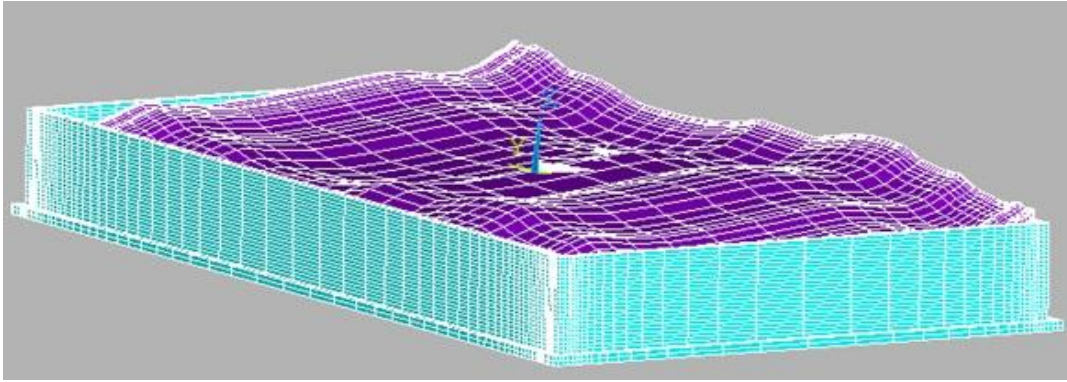


Figure 4.4. Free water surface profile at the moment the maximum sloshing occurs for a typical shallow tank

The amplification of wave height at the corner of the tank against the one at the middle of the wall is profoundly related to the tank configuration. If B and L , respectively, symbolize the length of the tank wall perpendicular and the one parallel to direction of the ground motion; the higher amplification at the corner relative to the middle of the wall happens for the case with smaller value of B/L ratio. For instance; the wave height at the corner of a square tank, with B/L ratio of 1.0, is increased by 75% in comparison with that at the middle of the wall.

4.2. Comparison of Sloshing height for 2D and 3D models

The differences between calculated sloshing height for 2D and 3D models as well as the effect of factor such as tank configuration and water depth are discussed in this section. It should be noted that, similarly, B and L , respectively, represent the length of the wall perpendicular and the wall parallel to the direction of the ground motion. In cases where the length to width ratio of the container is quite large, a 2D model based on the cross section perpendicular to the long side wall may be used to determine the sloshing response of the container for the ground motion acting parallel to the cross section. On the other hand, 3D modelling of the tanks represents a more realistic simulation of the tank behaviour and predicts higher values for the wave height at the middle of the short and long side wall in comparison with 2D models.

Among different tanks under investigation, the peak sloshing heights are presented for three cases of tall tanks. All of them have water depth of 11.0 m and the length of walls parallel to the direction of the ground motion in these three tanks is 40.0 m. These tanks are referred to as; T1, T2 and T3; respectively, with the corresponding lengths of the walls perpendicular to direction of ground motion equal to 40.0, 60.0 and 80.0 m, respectively. For case T1, the time history of sloshing height for both 2D and 3D models is shown in Fig. 4.5. Note that, B/L ratio for this case equals to 1.0. For the 3D model, the peak wave height at the middle cross section of the long side wall is 744 mm. This value is 22% higher than the value conducted by the 2D model.

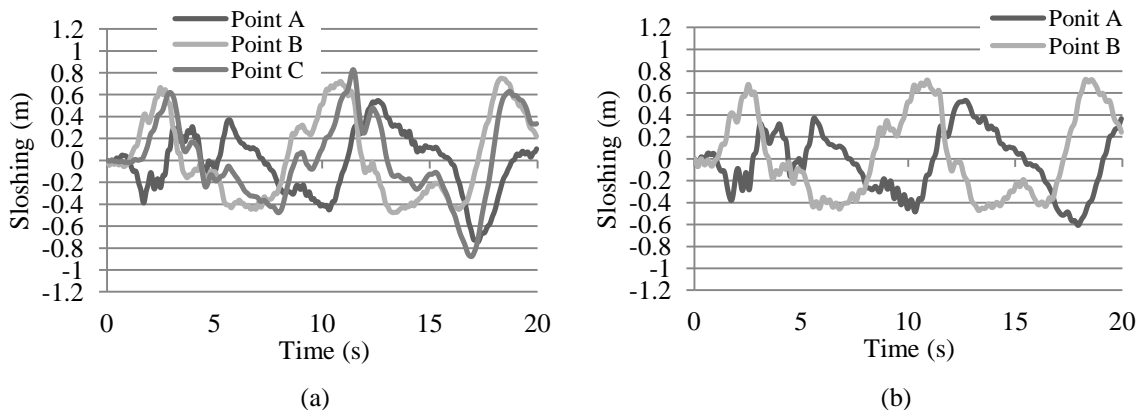


Figure 4.5. Time history of sloshing for case T1: (a) 3D model, (b) 2D model

For case T2, time histories of slosh height at critical points of both 3D and 2D models are shown in Fig. 4.6. Note that, the B/L ratio for case T2 is 1.5. For the 3D model of case T2, the peak wave amplitude at point A is 675 mm, similarly, it is 11% higher than the one of 2D model. Moreover, as is demonstrated in Fig. 4.7, for the 3D model of case T3, the sloshing height at point A is 666 mm and is 10% higher than the 608 mm slosh height obtained using the 2D model. The B/L ratio for case T3 is 2.0. It can be concluded that the three-dimensional geometry has a significant effect on the dynamic responses. The amplification of sloshing response of the 3D model in comparison with 2D response is significant for the case that has smaller value of B/L ratio.

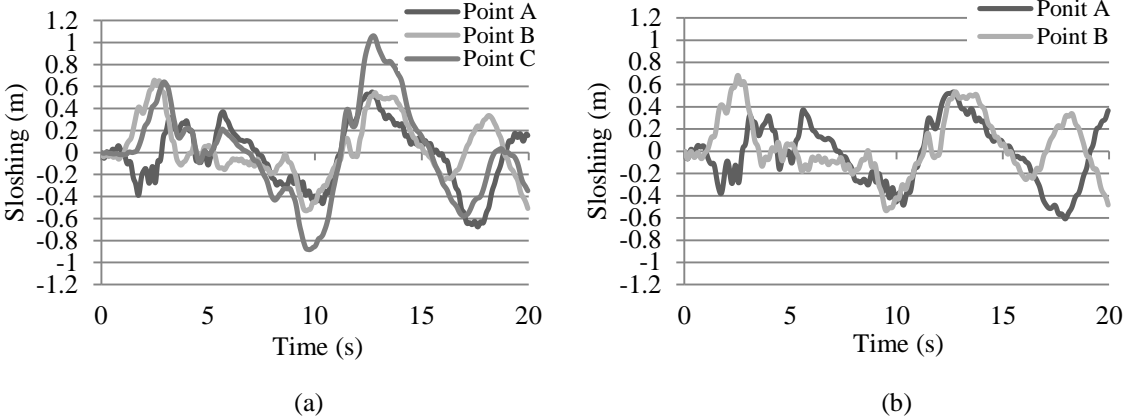


Figure 4.6. Time history of sloshing for case T2: (a) 3D model, (b) 2D model

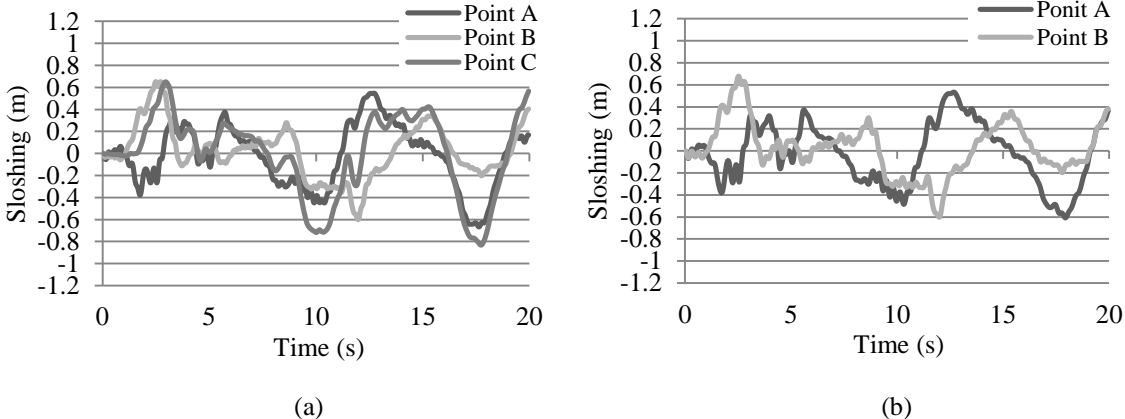


Figure 4.7. Time history of sloshing for case T3: (a) 3D model, (b) 2D model

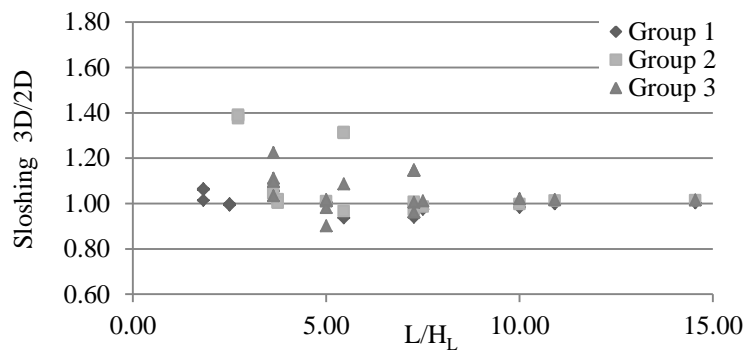
Additionally, comparisons are presented for three groups of rectangular tanks. The plan dimensions of the selected tank configuration in this study are summarized in table1, for different tank groups. In each group, tanks have water depth of 5.5, 8.0 and 11.0 m, which are referred to as shallow (S), medium (M) and tall (T) tank, respectively. The lengths of the tanks wall parallel to X direction are 20 m, 30 m and 40 m, for groups 1, 2 and 3, respectively. The dimensions of the other side walls also vary and each group contains of rectangular tanks with length of the walls parallel to Y direction equal to 40, 60 and 80 m.

In order to make a general statement, the sloshing height is calculated for all of the tanks summarized in Table 4.1, using both 2D and 3D models. Fig. 4.8 displays the increase in sloshing height in 3D models in comparison with the 2D models against L/H_L ratio. It can be concluded that, in general, 3D models estimate higher values for the sloshing height in comparison with the 2D models. It is observed that the effect of the walls parallel to the direction of the excitation cannot be ignored for the cases with smaller value for the B/L ratio. For these cases, the differences in wave height obtained from 3D and 2D models are more profound. The maximum difference between the results of 3D and 2D tank models are 12%, 40% and 22% for groups 1, 2 and 3, respectively.

Table 4.1. Plan dimension of the selected tank configurations for this study

	Case	2L _X (m)	2L _Y (m)	Case	2L _X (m)	2L _Y (m)	Case	2L _X (m)	2L _Y (m)
Group 1	S1-1	20	40	S1-2	20	40	S1-3	20	40
	M1-1	20	60	M1-2	20	60	M1-3	20	60
	T1-1	20	80	T1-2	20	80	T1-3	20	80
Group 2	S2-1	30	40	S2-2	30	40	S2-3	30	40
	M2-1	30	60	M2-2	30	60	M2-3	30	60
	T2-1	30	80	T2-2	30	80	T2-3	30	80
Group 3	S3-1	40	40	S3-2	40	40	S3-3	40	40
	M3-1	40	60	M3-2	40	60	M3-3	40	60
	T3-1	40	80	T3-2	40	80	T3-3	40	80

According to Fig. 4.8, it can be concluded that the sloshing response is very sensitive to L/H_L ratio. However, as this ratio reaches the value of 10, the response of the 3D models becomes very close to that of 2D models. A similar trend to sloshing response was reported by Kim et al. (1998). The graph also confirms that for the cases with smaller B/L ratio, there is a significant difference between 3D and 2D responses. For the tanks with ratio of B/L greater than 2.0, the response of 2D and 3D models approaches to similar value. This fact may justify the use of 2D models for the tanks that have B/L and L/H_L ratios greater than 2.0 and 10, respectively.

**Figure 4.8.** Relative sloshing height amplification against L/H_L

5. CONCLUSIONS

Calculation of the vertical displacement of the liquid is a matter of importance in design of the required free-board in LCS. It should be noted that the interaction of the generated waves at the corner of the rectangular tank causes a significant increase in sloshing heights; however, the two-dimensional models are unable to directly predict the behaviour of the system.

In this study, the finite element method is employed to predict the sloshing height of the water in seismically excited flexible rectangular tanks. The liquid sloshing is modelled considering appropriate boundary conditions. The damping effect is also introduced by the Rayleigh method. Liquid-tank system is modelled assuming both three-dimensional and two-dimensional geometries.

It is concluded that the wave amplitude at the corner of the three-dimensional tank is higher than the wave amplitude at the middle cross section of the walls. The amplification of wave height at the corner of the tank against the one at the middle of the wall is profoundly related to tank configuration as well as the water depth. If B and L, respectively, symbolize the length of the tank wall perpendicular and the one parallel to direction of the ground motion; the higher amplification at the corner relative to the middle of the wall happens for the case with smaller value of B/L ratio. The wave height at the corner of the square tank is increased up to 75% in comparison with the one at the middle of the wall. Moreover, in this study, it is observed that for the tanks of the same dimensions, the amplification of

slosh wave at the corner of the tank relative to the one at the middle of the wall is more profound for the tanks with greater water depth.

The three-dimensional modelling of the tanks represents a more realistic simulation of the tank behaviour and predicts higher values for the wave height. In this study, it is observed that the 3D modelling of the tanks resulted in higher values for the wave height in both X and Y direction to up to 40%, in comparison with 2D models.

It is concluded that the sloshing response is very sensitive to both L/H_L and B/L ratios. However, as L/H_L ratio reaches the value of 10, the response of the 3D models becomes very close to that of 2D models. In addition, it is observed that for the cases with smaller B/L ratio, there is a significant difference between 2D and 3D responses. For the tanks with ratio of B/L greater than 2.0, the response of 2D and 3D models approaches to similar value. This fact may justify the use of 2D models for the tanks that have B/L and L/H_L ratios greater than 2.0 and 10, respectively.

AKNOWLEDGEMENT

Financial support provided by the Natural Science and Engineering Research Council of Canada (NSERC) in the form of a discovery grant to the second author is greatly appreciated.

REFERENCES

- American Concrete Institute Committee 350. (2006). Seismic design of liquid-containing concrete structures (ACI 350.3-06) and commentary (350.3R-06), American Concrete Institute, Farmington Hills, Mich
- Chopra, A.K. (1995). Dynamics of structures, Prentice-Hall, Upper Saddle River, N.J.
- Dodge, F.T. (2000). The new dynamic behavior of liquids in moving containers, Southwest Research Institute, San Antonio, Texas
- Ghaemmaghami, A.R. Kianoush M.R. (2010). Effect of Wall Flexibility on Dynamic Response of Concrete Rectangular Liquid Storage Tanks under Horizontal and Vertical Ground Motion. *J. of Struct. Eng.* **136**:4,441-450
- Haroun, M.A. (1984). Stress Analysis of Rectangular Walls under Seismically Induced Hydrodynamic Loads. *Bull. Seismol. Soc. Am.* **74**:3,1031-1041.
- Haroun M.A., Housner G.W. (1981). Earthquake response of deformable liquid storage tanks. *ASME J. Appl. Mech.* **48**,411-418.
- Housner, G.W. (1957). Dynamic pressure on accelerated fluid containers. *Bull. Seismol. Soc. Am.* **47**:1,15-35.
- Housner, G.W. (1963). The dynamic behavior of water tanks. *Bull. Seismol. Soc. Am.* **53**:2,381-387.
- Ibrahim R.A., Pilipchuk V.N. (2001). Recent advances in liquid sloshing dynamics. *American Society of Mechanical Eng.* **54**:2,133-197.
- Karamanos, S.A. Patkas, L.A. and Platyrrachos, M.A. (2006). Sloshing effects on the seismic design of horizontal-cylindrical and spherical industrial vessels. *ASME J. Pressure Vessel Technol.* **128**:3,328-340.
- Kim, J.K., Koh H.M. and Kwahk I.J. (1996). Dynamic response of rectangular flexible fluid containers. *J. Eng. Mech.* **122**:9,807-817.
- Koh, H.M., Kim J.K. and Park J. H. (1998). Fluid-structure interaction analysis of 3D rectangular tanks by a variationally coupled BEM-FEM and comparison with test results. *Earthqu. Eng. Struct. Dyn.* **27**,109-124.
- Livaoglu, R. (2008). Investigation of seismic behavior of fluid rectangular tank-soil/foundation systems in frequency domain. *Soil Dyn. Earthquake Eng.* **28**:2,132-146.
- Subhash Babu, S. and Bhattachryya S.K. (1996). Finite element analysis of fluid-structure interaction effect on liquid retaining structures due to sloshing. *Computer & Structures* **59**:6,1165-1171.
- Tavakkoli Avval, I., Kianoush M.R. and Ghaemmaghami A.R. (2012). Sloshing Characteristic of Rectangular Concrete Tanks under Seismic Loading. *Proc. 3rd Int. Struct. Specialty Conference*. Edmonton, Alberta
- Veletsos, A.S. Tang Y. and Tang H.T. (1992). Dynamic response of flexibly supported liquid storage tanks, *J. Struct. Engineering* **118**,264-283.
- Virella, J.C., Prato C.A. and Godoy L.A. (2008). Linear and nonlinear 2D finite element analysis of sloshing modes and pressure in rectangular tanks subjected to horizontal harmonic motions. *J. Sound Vibration.* **312**:3,442-460.
- Wald, D.J., Kanamori, Hiroo, Helmberger, D.V. and Heaton, T.H. (1993). Source study of the 1906 San Francisco Earthquake. *Bulletin of the Seismological Society of America* **83**:4,981-1019
- Zienkiewicz, O.C. (1977). The Finite Element Method, McGraw-Hill Company, London.